

# Robustness against parametric noise of non ideal holonomic gates

Cosmo Lupo, Paolo Aniello, and Mario Napolitano  
*Università “Federico II” and INFN, Sezione di Napoli, I-80126 Napoli, Italy*

Giuseppe Florio  
*Università di Bari and INFN, Sezione di Bari, I-70125 Bari, Italy*

Holonomic gates for quantum computation are commonly considered to be robust against certain kinds of parametric noise, the very motivation for this robustness being the geometric character of the transformation achieved in the adiabatic limit. On the other hand, the effects of decoherence are expected to become more and more relevant when the adiabatic limit is approached. Starting from the system described by Florio *et al.* [Phys. Rev. A **73** 022327 (2006)], here we discuss the behavior of non ideal holonomic gates at finite operational time, i.e., far before the adiabatic limit is reached. We have considered several models of parametric noise and studied the robustness of finite time gates. The main result is that the issue of robustness is problematic and may strongly depend on some features of the noise such as its symmetries and typical frequencies.

PACS numbers: 03.67.Lx, 03.65.Vf, 03.65.Yz

## I. INTRODUCTION

One of the most important challenges for the realization of quantum information tasks is the implementation of quantum logic gates that are *robust* against unwanted perturbations [1, 2]. Two kinds of perturbations with qualitatively different features can be distinguished: the first kind has a purely *quantum* nature, and it is induced by the interaction of the quantum system implementing the logic gate with the environment; the second kind has instead a *classical* nature, and it is caused by the presence of instrumental noise in the ‘external parameters’ used to control the system. The unwanted interaction with the environment is the source of the phenomenon known as quantum *decoherence* [3]. The effects of this interaction can be modeled by means of suitable ‘master equations’ (i.e. evolution equations) for the density matrix of the quantum system implementing the logic gate; they are negligibly small if the *operational time* of the logic gate is short enough. The classical perturbations stem from an unavoidable noisy component intrinsic in the external driving fields (e.g. laser beams [4]) that can be usually regarded as classical fields; hence, it is essentially due to instrumental instability. The effects of these perturbations can be evaluated by studying standard (non-autonomous) Schrödinger equations where the instrumental noise is taken into account by suitably modeling the noisy components of the classical parameters (e.g. the field amplitude) associated with the external driving fields.

Among the several strategies for realizing quantum logic gates discussed in the literature, a prominent position is held by *holonomic gates*. They were first proposed by Zanardi and Rasetti [5] (see also Ref. [6]), and rely on the theory of holonomy and of the associated holonomy groups in principal fiber bundles [7], a subject which is familiar to theoretical physicists due to the central role played in gauge theories [8] and in the well-known phenomenon of abelian [9] and non-abelian [10] adiabatic phases. Actually, a holonomic gate can be regarded as a straightforward application of the theory of non-abelian adiabatic phases to quantum computation.

Since the very beginning, holonomic gates were considered

to be intrinsically robust against classical noise [11], thanks to the geometric features of holonomy in Hilbert bundles. As we will briefly recall below, three main ingredients are needed in order to realize such holonomic gates.

The first ingredient is a suitable physical system described by a quantum Hamiltonian depending on some set of parameters, these parameters being associated with the external (classical) driving fields that are assumed to be experimentally controllable functions of time; the unavoidable instrumental instability (stochastic noise) affecting the driving fields is the source of the kind of classical noise — we will call it *parametric noise*, in the following — that has been mentioned above.

The second ingredient consists in selecting a suitable eigenspace of the given Hamiltonian — an eigenspace depending smoothly on the external parameters, hence actually an iso-degenerate family of eigenspaces; let us call them the family of *relevant eigenspaces* — and in fixing in the parameter space an ‘initial point’ and a loop through this point. To such a loop corresponds an excursion of the parameter-dependent Hamiltonian (hence, of its eigenprojectors) and a certain *ideal unitary transformation* in the *encoding eigenspace*, namely, that particular relevant eigenspace fixed by the initial (and final) point of the loop in the parameter space. This ideal transformation is determined by *Kato’s adiabatic evolver* associated with the given Hamiltonian and with the chosen loop in the parameter space, and it has a simple geometric interpretation as a holonomy phenomenon (geometric phase). The ideal unitary transformation plays a central role in Kato’s formulation of the adiabatic theorem [12] applied to our context. Indeed, the external parameters are controllable functions of time and in the *adiabatic limit* — i.e., in the limit where the loop in the parameter space is covered in a operational time tending to infinity — the *real evolution over the operational time*, determined by the given physical Hamiltonian, becomes *cyclic* in the encoding eigenspace and, apart from an irrelevant overall ‘dynamical phase factor’, *coalesces in this subspace with the ideal unitary transformation*. We stress that the ideal unitary transformation should be thought, in our context, as an *ideal quantum gate* whose behavior can be, in general, only approached by a *non-ideal quantum gate*

corresponding to the real evolution over a suitably large, but finite, operational time.

Accordingly, the third ingredient is the choice of a suitable operational time — which will be called *balanced working time*, in the following — for the real quantum gate. This time span must be short enough to achieve a fast quantum computer and to avoid the ravages of decoherence, but long enough to justify the adiabatic approximation (i.e. to approach the behavior of the ideal quantum gate) which is at the root of the appearing of geometric phases [33]. Hence, a balanced working time is determined by a touchy trade-off between two competing and not necessarily compatible demands.

The problem of robustness of holonomic gates against parametric noise has been studied both in the abelian [15] and in the non-abelian case [16]. In these papers, the effects of random perturbations of the control parameters are considered. It is worth noticing, however, that such effects are evaluated with the adiabatic limit already being performed, thus essentially confirming quantitatively the standard qualitative *geometric argument* usually adopted to support the robustness of holonomic gates, argument which will be recalled later on. We emphasize that, on the other hand, the operational time (in particular, the balanced working time) of a quantum gate is obviously always finite; hence, in principle, *the mentioned geometric argument could generally not apply to concrete devices*. A critical analysis of this simple, but somewhat subtle, issue is the main aim of the present contribution.

As holonomic gates are generally considered to be *a priori* robust against parametric noise, attention has mainly focused on the study of decoherence effects [17, 18, 19, 20] and on the possibility of partially suppressing them [21]. These investigations show that for certain physical systems, and for certain models and regimes of the coupling with the environment, one is able to estimate the typical time-scale within which the effects of decoherence can be neglected. Hence one can determine, in principle, a balanced working time for these systems. At this point, according to what has been observed above, one should actually *check* whether this balanced working time guarantees a suitable robustness of the quantum gate against parametric noise, namely, whether the effects of this kind of noise on the fidelity of the non-ideal quantum gate with respect to the ideal one can be neglected or not.

Recently, a new ingredient has been proposed for the implementation of a holonomic quantum gate [22] (see also [23, 24]). Indeed, some authors have observed — for the model of a ion-trap quantum gate proposed by Duan *et al.* [25], model which is also central in the present contribution — the existence of a *optimal working time*, namely, of a specific operational time for which the non-ideal (i.e. finite-time) gate behaves *exactly* as the ideal (i.e. adiabatic) gate; they show, furthermore, that over the optimal working time the effects of the environment are negligible. Thus, such a optimal working time turns out to be also a balanced working time.

Again we stress that, anyway, the fact that the non-ideal gate behaves, in correspondence to the optimal working time, as the ideal one cannot be used to rule out the influence of parametric noise on the base of the standard geometric argument. Indeed, one should not expect that, perturbing the loop in the

parameter space, the non-ideal gate will still mimic the behavior of the ideal one. Hence, once again, one cannot apply, in principle, the standard geometric argument to support the robustness of this kind of holonomic gate against parametric noise.

In conclusion, we think that the impact of parametric noise on holonomic gates is still an open problem and one is not legitimated, in general, to state the robustness of non-ideal holonomic gates against this kind of perturbations on the base a generic geometric argument. In our present contribution, we will try to illustrate this assertion by means of quantitative arguments, focusing on the ion-trap model proposed by Duan *et al.* [25]. Even if other models have been proposed in the literature [26], the model of Duan *et al.* is probably the one most extensively studied also with reference to different physical systems, as Josephson junctions [27] and semiconductor quantum dots [28], and can be regarded as a reference point for the subject.

The paper is organized as follows. In Sec. II holonomic quantum logical gates are discussed starting from the point of view of Kato's proof of the adiabatic theorem. In Sec. III the model Hamiltonian is introduced which will serve as a case study. In Sec. IV the behavior of the considered system in presence of several models of parametric noise is discussed. Conclusions and comments are presented in Sec. V.

## II. ADIABATIC VERSUS FINITE TIME GATES

The main aim of this section is to review critically the standard argument that is used in the literature in order to support the robustness of holonomic gates against noise. As already stressed in the introduction, non-ideal holonomic gates — i.e., holonomy-based devices that can be concretely realized in a laboratory — must necessarily have a finite working time which should be short enough in order to avoid the perturbing effects of decoherence. This issue has been carefully analyzed in a recent paper [22], where it is shown explicitly, on the base of a concrete model of adiabatic holonomic gate, that decoherence effects can prevent the possibility of achieving a faithful holonomic gate when the adiabatic limit is approached. This result is coherent with theoretical speculations (see Ref.s [29, 30]) on the failure of the adiabatic theorem in presence of dissipative terms in the master equation governing the dynamics of the physical system implementing the quantum gate.

In [22, 23] it has been also shown that there may exist *specific* operational times ('optimal working times') for non-ideal holonomic gates allowing to obtain a high fidelity together with a good robustness against decoherence. It is then worth studying the robustness of non-ideal holonomic gates against instrumental noise.

As a first step, we will consider the classical Kato's proof of the adiabatic theorem [12]. This proof was originally formulated in order to go beyond some limitations imposed by previous proofs [31], such as the requirement of a Hamiltonian with *non-degenerate* eigenvalues. However, the most remarkable idea in Kato's proof is the introduction of an *ideal*

*evolution operator* — that we may call the ‘Kato evolutor’ — reproducing the typical adiabatic behavior of a quantum system; one can then prove that, under suitable hypotheses, in the proper limit the *real* evolution of the quantum system *coalesces* with the ideal adiabatic evolution.

In the standard construction of holonomic gates, a quantum system is considered with a Hamiltonian which depends on points  $\mathbf{r}$  on a suitable manifold  $\mathcal{M}$ . For the sake of simplicity, here we consider the case in which the family of Hamiltonians  $H(\mathbf{r})$  is isodegenerate with a pure discrete spectrum. A local set of coordinates  $\{x^\mu\}$  on  $\mathcal{M}$  plays the role of parameters that are supposed to be experimentally controllable. The control parameters are allowed to perform a cyclic evolution in the operational time  $\tau$

$$\gamma \mid t \in [0, \tau] \longrightarrow \mathbf{r}(t), \quad (1)$$

with  $\mathbf{r}(\tau) = \mathbf{r}(0)$ .

As usual we define  $s \equiv t/\tau$ , in terms of this parameter the Schrödinger equation reads as follows:

$$\psi'_\tau(s) = -i\tau H(\mathbf{r}(s))\psi_\tau(s), \quad s \in [0, 1], \quad (2)$$

where we have re-defined  $\mathbf{r}(s) \equiv \mathbf{r}(s\tau)$ . Here and in the following  $X'(s) \equiv dX(s)/ds$ .

In view of the case study that will be considered below, we restrict our discussion to the special case in which the distinct eigenvalues of  $H(\mathbf{r}(s))$  are a finite set and do not depend on time. In these hypotheses, the time dependent Hamiltonian has a spectral decomposition

$$H(\mathbf{r}(s)) = \sum_{l=0}^{n-1} \lambda_l P_l(s). \quad (3)$$

Where  $\lambda_l$  are all distinct eigenvalues and  $P_l(s)$  are the corresponding instantaneous eigenprojectors, we also assume that the eigenprojectors are at least piecewise twice continuously differentiable for  $s \in [0, 1]$ . In the following we pick up one eigenprojectors, say  $P_0$ , that corresponds to the computational subspace that will be introduced below. In order to neglect an overall phase factor the dynamical contribution to the adiabatic transformation and to simplify the notation we set  $\lambda_0 = 0$  and rename  $P(s) \equiv P_0(s)$ .

The solution of the Schrödinger equation (2) reads

$$\psi_\tau(s) = V_\tau(s)\psi_\tau(0). \quad (4)$$

$V_\tau(s)$  is the unitary operator which describes the dynamical transformation that obeys:

$$V'_\tau(s) = -i\tau H(\mathbf{r}(s))V_\tau(s), \quad (5)$$

with the initial condition  $V_\tau(0) = \mathbb{I}$ .

On the other hand, the adiabatic transformation is defined as a solution of the equation

$$U'(s) = iA(s)U(s), \quad (6)$$

where

$$iA(s) = [P'(s), P(s)] = P'(s)P(s) - P(s)P'(s). \quad (7)$$

The solution of (6) is completely determined once the initial condition is given. The solution  $U(s)$ , with the initial condition  $U(0) = \mathbb{I}$ , is unitary and has the property

$$P(s)U(s) = U(s)P(0). \quad (8)$$

This last relation indicates that  $U(s)$  transforms isometrically the eigenprojector at initial time  $P(0)$  onto the instantaneous eigenprojector  $P(s)$ . In order to look closely at the computational space, we consider the operator

$$W(s) \equiv U(s)P(0), \quad (9)$$

since  $W(s)P(0) = U(s)P(0)$ ,  $U(s)$  is equivalent to  $W(s)$  when restricted on functions of the eigenprojector  $P(0)$ . It is easy to see that  $W(s)$  obeys the simpler equation (compare with (6))

$$W'(s) = P'(s)W(s). \quad (10)$$

The adiabatic theorem states that the dynamical transformation, restricted to the eigenspace with eigenprojector  $P(0)$ , asymptotically approaches the adiabatic transformation. Defining  $W \equiv W(1)$  and  $V_\tau \equiv V_\tau(1)$ , the following relation holds [12]:

$$[V_\tau - W]P(0) = iV_\tau \sum_{l \neq 0} \frac{\Delta_l(\tau)}{\lambda_l \tau}, \quad (11)$$

where

$$\Delta_l(\tau) = [V_\tau^\dagger(s)P_l(s)W'(s)]_0^1 - \int_0^1 d\sigma V_\tau^\dagger(\sigma) (P_l(\sigma)W'(\sigma))' \quad (12)$$

It is easy to show [12] that the operators  $\Delta_l(\tau)$  are bounded uniformly with respect to  $\tau$ . Choosing a suitable operator norm  $\|V_\tau \Delta_l(\tau)\| \leq M$ , and

$$\|[V_\tau - W]P(0)\| \leq M \sum_{l \neq 0} \frac{1}{|\lambda_l \tau|}. \quad (13)$$

Notice that  $\Delta_l(\tau)$  depend on the gate operational time  $\tau$  through the unitary operator  $V_\tau(s)$ . Thus we can expect, before the asymptotic limit, an oscillatory behavior of a suitably defined gate fidelity as a function of  $\tau$ . The fidelity revivals described in [22] are a particular case of this general oscillatory behavior at finite operational time.

Equation (10) defines a notion of parallel transport which corresponds to the adiabatic transformation. Let us choose a basis  $\{\psi_\alpha(s)\}$  in the instantaneous subspace ( $P(s) = \sum_\alpha |\psi_\alpha(s)\rangle\langle\psi_\alpha(s)|$ ). The adiabatic connection is defined as follows [10]:

$$A \equiv A_{\alpha\beta}(s) = \langle\psi_\beta(s)| \frac{d}{ds} \psi_\alpha(s) \rangle \quad (14)$$

The adiabatic transformation at the end of a loop in the parameter manifold can be written as  $W = W_{\alpha\beta}|\psi_\beta(1)\rangle\langle\psi_\alpha(1)|$  and it is given by the corresponding holonomy:

$$W = \mathbf{P} \exp \int_\gamma A ds, \quad (15)$$

where  $\mathbf{P}$  stands for the path ordered product. In a local chart  $Ads = A_\mu dx^\mu$ . By means of the (in general non Abelian) Stokes' theorem, the holonomy is determined by the curvature tensor, whose component expression is

$$F_{\mu\nu} = \partial_\nu A_\mu - \partial_\mu A_\nu - [A_\mu, A_\nu]. \quad (16)$$

In most of the applications for quantum information tasks, (15) reduces to a simple exponential and the Abelian version of the Stokes' theorem can be applied:

$$W = \exp \int_C F_{\mu\nu} dx^\mu \wedge dx^\nu, \quad (17)$$

where  $C$  is a region whose boundary is the loop  $\gamma$ . The usual argument in favor of the robustness of holonomic gates follows directly from expression (17). Since the integral of the curvature is supposed to depend weakly on the details of the loop, the adiabatic transformation is considered to be robust against a *geometrical* perturbation in the closed path  $\gamma$ .

To conclude this section, we emphasize that what is really needed in order to obtain a transformation with a geometrical character is a cyclic evolution of the eigenspace ( $P(1) = P(0)$ ). The adiabatic theorem ensures that this cyclic evolution appears in correspondence with a loop in the parameters manifold in the adiabatic limit. Only in this limit the transformation can be considered purely geometric and the argument of robustness holds.

### III. A CASE STUDY

As a case study, here we consider the single-qubit non Abelian gate that was proposed in [25]. The model under consideration can be physically realized as, for instance, a trapped ion with two degenerate ground (or metastable) states  $|0\rangle$  and  $|1\rangle$  which play the role of the computational basis. A quasi degenerate ancillary state  $|a\rangle$  and an excited state  $|e\rangle$  are also needed (the scheme is drawn in Fig. 1(a)). The low energy states are supposed to be independently coupled with the excited state, such that the interaction picture Hamiltonian in the rotating frame reads as follows:

$$H(\mathbf{r}) = H(x, y, z) = |e\rangle [x\langle 0| + y\langle 1| + z\langle a|] + \text{h.c.} \quad (18)$$

The real parameters  $x, y, z$  are related to three independent Rabi frequencies corresponding to resonant laser beams with different energies and polarization. In an ideal experiment these parameters are constrained to take values on a two-sphere, it is thus convenient to introduce polar coordinates:

$$\begin{cases} x = \Omega \sin \vartheta \cos \varphi \\ y = \Omega \sin \vartheta \sin \varphi \\ z = \Omega \cos \vartheta \end{cases} \quad (19)$$

The spectrum of (18) is threefold:  $\sigma = \{0, \pm\Omega\}$ , with the null eigenvalue which is doubly degenerate. The two degenerate eigenstates with vanishing energy can be chosen as follows:

$$\begin{aligned} |\psi_0\rangle &= \cos \vartheta (\cos \varphi |0\rangle + \sin \varphi |1\rangle) - \sin \vartheta |a\rangle, \\ |\psi_1\rangle &= -\sin \varphi |0\rangle + \cos \varphi |1\rangle. \end{aligned} \quad (20)$$

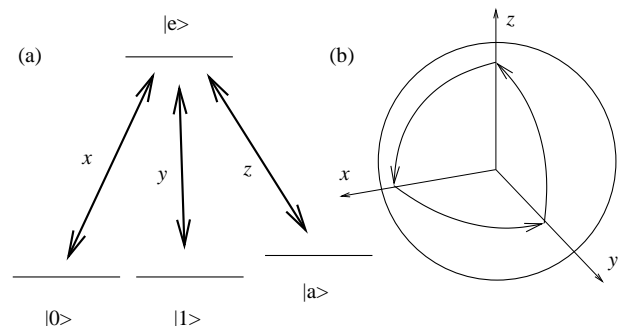


FIG. 1: Structure of the atomic levels and resonant lasers (a); unperturbed loop (21) in the parameter manifold (b).

An analysis of the holonomy associated to the Hamiltonian (18) in correspondence with the doubly degenerate subspace shows that a closed path with starting point  $\vartheta = 0$  corresponds to a non Abelian holonomy  $W = \exp[-i\sigma_y\omega]$ , where  $\sigma_y = -i(|0\rangle\langle 1| - |1\rangle\langle 0|)$  is the Pauli matrix in the computational space and  $\omega$  is the solid angle swept by the parameter  $\vartheta(s)$  and  $\varphi(s)$ . Here we consider the closed path in the parameter manifold that was studied in [22]. For  $s \in [0, 1]$  we take (see Fig. 1(b)):

$$\begin{aligned} \vartheta(s) &= \begin{cases} 3s\pi/2 & s \in [0, 1/3] \\ \pi/2 & s \in [1/3, 2/3] \\ 3\pi/2(1-s) & s \in [2/3, 1] \end{cases} \\ \varphi(s) &= \begin{cases} 0 & s \in [0, 1/3] \\ 3\pi/2(s - \frac{1}{3}) & s \in [1/3, 2/3] \\ \pi/2 & s \in [2/3, 1] \end{cases} \end{aligned} \quad (21)$$

The solid angle related to the loop (21) is  $\omega = \pi/2$ , hence the corresponding holonomic gate is  $W = -i\sigma_y$ . Notice that some care is needed in the calculation of the integral (15) since the basis (20) is ill defined at the north pole.

As was observed in [22], the remarkable property of this path is that it presents perfect revivals of the gate fidelity at finite operational time. The same behavior was predicted for all the loops constructed by moving from the north pole to the equator through a meridian and back to the north pole through another meridian with piecewise constant velocity. In the case of the loop (21) there is a unity gate fidelity in correspondence of the operational times:

$$\tau_k^* = \frac{3\pi}{2\Omega} \sqrt{16k^2 - 1}, \quad k = 1, 2, \dots \quad (22)$$

In the following we are mostly concerned with the first optimal operational time  $\tau^* \equiv \tau_1^*$ .

To conclude this section we notice that a perfect revival of fidelity at finite operational time corresponds to the phase acquired in correspondence to a non adiabatic *cyclic* dynamics [13, 14]. In particular, for our case study, it happens that, in correspondence to an optimal operational time, the evolution becomes cyclic and the acquired geometric phase is equal to the adiabatic holonomy.

#### IV. MODELS OF NOISE

In order to study the robustness of non ideal holonomic gates, we consider the response of the system under parametric noise in the ideal loop (21). In order to quantify the robustness of the gate, the noisy finite time evolution of the system is solved with analytic or numerical methods and the average gate fidelity is calculated. In the following, several models of noise are taken into account: in Sec. IV A we consider the response of the system under a monochromatic perturbation of the three Rabi frequencies in (18); in Sec. IV B we consider a model of noise expressed by a random step function in the angular variables (19) on the sphere; finally, in Sec. IV C we discuss the response of the system under a random perturbation in the three Rabi frequencies.

##### A. Monochromatic noise

In this section we consider the behavior of the system in presence of a parametric noise with only one monochromatic component. A generic noisy path can be written as follows:

$$\mathbf{r}_n(t) = \mathbf{r}(t) + \boldsymbol{\epsilon}(t), \quad t \in [0, \tau], \quad (23)$$

where  $\mathbf{r}(t)$  is the unperturbed loop and  $\boldsymbol{\epsilon}(t)$  is a random function which is specified, for each component, by its power spectrum, i.e., the square modulus of the Fourier transform:

$$S(\eta) = |\boldsymbol{\epsilon}(\eta)|^2, \quad (24)$$

where

$$\boldsymbol{\epsilon}(t) = \int d\eta \boldsymbol{\epsilon}(\eta) e^{i\eta t}. \quad (25)$$

The random character of  $\boldsymbol{\epsilon}(t)$  corresponds to the randomness of  $\arg[\boldsymbol{\epsilon}(\eta)]$ . Here we consider only one monochromatic component

$$\boldsymbol{\epsilon}(t) = \boldsymbol{\epsilon}(\eta) e^{i\eta t} + \boldsymbol{\epsilon}(-\eta) e^{-i\eta t}, \quad (26)$$

that can be re-written as follows:

$$\boldsymbol{\epsilon}(t) = \epsilon_\eta \sin(\eta t + \phi), \quad (27)$$

where  $\epsilon_\eta$  is real and  $\phi$  are random phases. Notice that taking the re-parametrization  $t \rightarrow s = t/\tau$  one obtains:

$$\boldsymbol{\epsilon}(s) = \epsilon_\eta \sin(\eta\tau s + \phi). \quad (28)$$

Let us come back to our case study. One can assume that a realistic source of parametric noise is due to the non perfect control of the three independent Rabi frequencies. We have chosen a monochromatic noise at frequency  $\eta$  and considered a noisy path obtained from (19) and (21):

$$\begin{cases} x_n(s; \eta, \epsilon_\eta, \tau, \phi_1) = x(s) + \epsilon_\eta \sin(\eta\tau s + \phi_1) \\ y_n(s; \eta, \epsilon_\eta, \tau, \phi_2) = y(s) + \epsilon_\eta \sin(\eta\tau s + \phi_2) \\ z_n(s; \eta, \epsilon_\eta, \tau, \phi_3) = z(s) + \epsilon_\eta \sin(\eta\tau s + \phi_3) \end{cases}, \quad (29)$$

where  $\phi \equiv (\phi_1, \phi_2, \phi_3)$  are random phases and  $\mathbf{r}_n(s) \equiv (x_n(s), y_n(s), z_n(s))$ . So we have:

$$\mathbf{r}_n(s) = \mathbf{r}(s) + \epsilon_\eta \sin(\eta\tau s + \phi), \quad s \in [0, 1]. \quad (30)$$

From this last relation it is clear that at finite operational time the perturbation does not reduce to a geometric perturbation of the loop in the parameters space since the perturbed path itself depends on the operational time. In presence of noise, different values of the operational time  $\tau$  correspond to different loops in the parameters manifold.

For given values of  $\eta, \epsilon_\eta, \tau$  and  $\phi_i$ , we consider the solution of the Schrödinger equation

$$V'_\tau(s; \eta, \epsilon_\eta, \phi) = -i\tau H(\mathbf{r}_n(s)) V_\tau(s; \eta, \epsilon_\eta, \phi), \quad s \in [0, 1]. \quad (31)$$

where, in presence of noise, the rescaled Hamiltonian  $H(\mathbf{r}_n(s))$  is dependent on  $\tau$ . Since we are mainly interested in the transformation emerging at the end of the loop, we set  $V_\tau(\eta, \epsilon, \phi) \equiv V_\tau(1; \eta, \epsilon_\eta, \phi)$ .

Notice that, for all practical purposes, taking the average over the random phases corresponds to the action of the completely positive map

$$\rho \longrightarrow \mathcal{E}(\rho) = \frac{1}{(2\pi)^3} \int d\phi V_\tau(\eta, \epsilon, \phi) \rho V_\tau(\eta, \epsilon, \phi)^\dagger. \quad (32)$$

This completely positive map has to be compared with the ideal adiabatic unitary dynamics, to do that, we have evaluated the average gate fidelity

$$F = \int d\psi \langle \psi | W^\dagger \mathcal{E}(|\psi\rangle\langle\psi|) W | \psi \rangle, \quad (33)$$

where  $d\psi$  indicates the normalized Fubini-Study metric in pure states. This was computed by means of the formula [32]:

$$F = \frac{1}{3} + \frac{1}{12} \text{tr} [W W^\dagger \mathcal{E}(P_0(0))] + \frac{1}{12} \sum_{j=1}^3 \text{tr} [W \sigma_j W^\dagger \mathcal{E}(\sigma_j)] \quad (34)$$

where  $\sigma_j$  are the Pauli matrices in the computational subspace.

For several values of  $\eta, \epsilon_\eta$  and  $\phi_i$ , Eq. (31) is numerically solved using the relation:

$$V_\tau(\eta, \epsilon, \phi) = \lim_{N \rightarrow \infty} \overleftarrow{\prod}_{k=0 \dots N} \exp \left[ -i\tau H(\mathbf{r}_n(k/N)) \frac{1}{N} \right] \quad (35)$$

Where  $\overleftarrow{\prod}$  stands for the path ordered product. The effective completely positive map (32) is evaluated taking the average over 50 random choices of the phases  $\phi_i$ . Figure 2 shows the estimated gate fidelity (34) plotted as a function of the adimensional operational time  $\Omega\tau$ , for several values of the noise amplitude and frequency. The unperturbed dynamics corresponds to  $\epsilon = 0$  and can be compared with the analytical results in [22], it exhibits perfect revivals of the average gate fidelity at finite time, in particular the first optimal operational time is  $\Omega\tau^* \simeq 18.24$ . The numerical results show that the pattern of gate fidelity as a function of the operational time can be completely different in presence of noise.

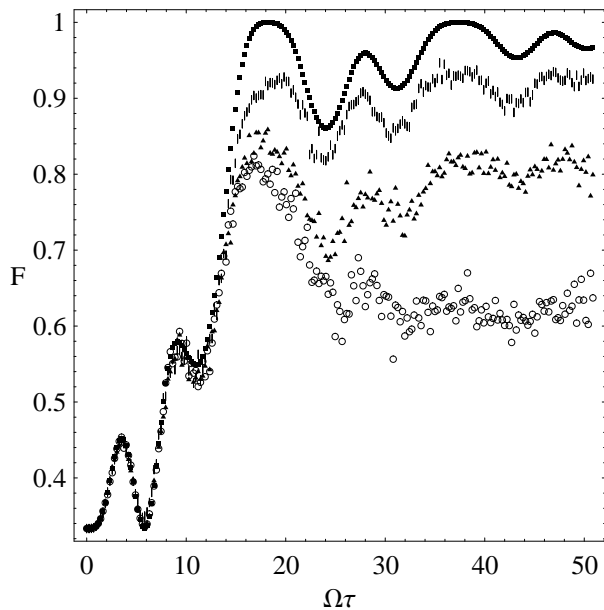


FIG. 2: Average gate fidelity as a function of the adimensional operational time  $\Omega\tau$  for several noise frequencies for the model in Sec. IV A. Boxes:  $\epsilon = 0$ , dashes:  $\epsilon = 0.1\Omega, \eta = 0.10\Omega$ , circles:  $\epsilon = 0.1\Omega, \eta = 0.18\Omega$ , triangles:  $\epsilon = 0.1\Omega, \eta = 0.19\Omega$

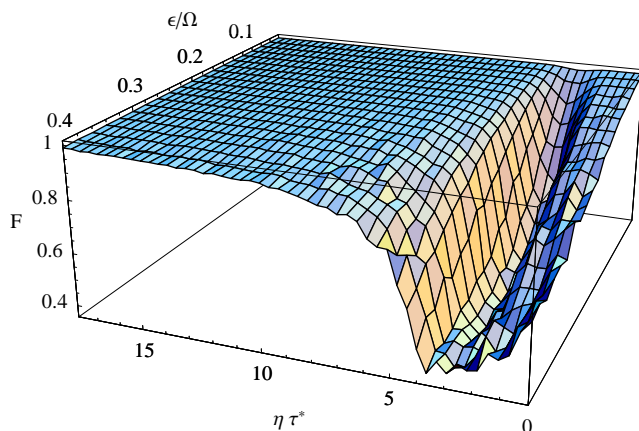


FIG. 3: (Color on line.) Average gate fidelity at the first optimal operational time as a function of adimensional noise frequency and amplitude for the model in Sec. IV A

The average gate fidelity at the first optimal operational time  $\Omega\tau^*$  in presence of parametric noise is plotted in Fig. 3 as a function of both amplitude and frequency of the noise. This plot shows that the gate is indeed robust also for rather large noise amplitude ( $\epsilon = 0.4\Omega$ ). This is true unless the noise frequency is in a particular range approximatively about  $\eta\tau^* \simeq 2.7$ , that corresponds to  $\eta \simeq 0.15\Omega$ .

We have also studied, with the same methods, the response of the system in presence of a noise which is square wave shaped. In this case a *probe* function is identified by its half period and initial phase. The corresponding patterns of the average gate fidelity are exactly analogous to the case of sinu-

soidal probe function.

Analogous results are also found for other loops of the same kind, such as the loop with the angle  $\varphi$  varying from 0 to  $\pi/4$  in (21) which is related to the Hadamard gate.

## B. Random noise on the sphere

In this section we consider a model of noise which preserves the spectrum of the unperturbed Hamiltonian (18), because of its symmetries an analytical solution of the noisy dynamics will be available.

In [22] it was shown that the evolution operator can be evaluated without approximation in several situations. Referring to the model in Eq. (18), it is possible to evaluate the evolution operator along *any* segment on the parametric sphere as far as one of the parameters ( $\vartheta, \varphi$ ) is kept constant. In particular, referring to the case in Fig. 1(b), the loop is composed by three segments and along each of them the previous condition is satisfied. Thus one can demonstrate [22] that the total evolution operator can be splitted in the form

$$U(\tau) = U_3(\tau_3)U_2(\tau_2)U_1(\tau_1), \quad (36)$$

where  $\tau$  is the total time evolution and  $\tau_i, i = 1, 2, 3$  are the times needed for covering each segment (for simplicity we suppose that the speed of the evolution are constant in each segment); moreover, the intermediate  $U_i$ 's can be explicitly calculated [22]. Their form is very peculiar and it is possible to see that, in terms of the parameters ( $\vartheta, \varphi$ ), one can write

$$U_1(t_1) = U_1(\vartheta_1(t_1), \varphi_1), \quad (37)$$

$$U_2(t_2) = U_2(\vartheta_2, \varphi_2(t_2)), \quad (38)$$

$$U_3(t_3) = U_3(\vartheta_3(t_3), \varphi_3), \quad (39)$$

where  $0 \leq t_i \leq \tau_i$  and  $\varphi_1, \vartheta_2$  and  $\varphi_3$  are the constant values of the parameters during the evolution along the segment 1, 2 and 3 respectively.

We want to use these results for gaining information about the influence of the noise. We will therefore consider the following model: every  $U_i$  is splitted in  $N$  evolution operators  $U_i^j$  evolving for a time  $\tau_{\text{step}} = \tau_i/N$  (a sub-segment); the evolution in the segment  $i$  reads

$$U_i(\tau_i) = \prod_{j=1}^N U_i^j(\tau_{\text{step}}). \quad (40)$$

In each sub-segment one of the sphere parameters is constant and the other evolves (we are moving on meridians or parallels). We add a random component to the constant parameter while the other is not affected. In other words, we are including a transverse component. We also suppose that the transverse evolution operator is equal to the identity (the “switch” is infinitely fast). This way we have splitted the evolution on a single meridian (parallel) in a sequence of evolutions on shorter meridians (parallels). Using Eq.s (37)-(40) we can

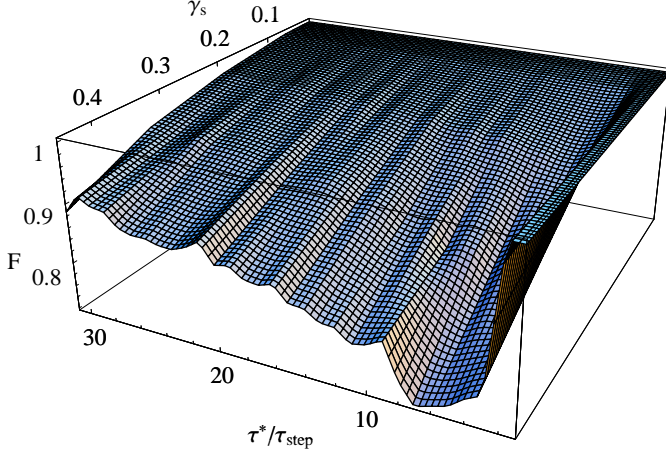


FIG. 4: (Color on line.) Average gate fidelity at the first optimal operational time as a function of the rescaled noise amplitude  $\gamma_s = \gamma/(\pi/2)$  and the ratio  $\tau^*/\tau_{\text{step}}$  for the model in Sec. IV B.

write

$$U_1(\tau_1) = \prod_{j=1}^N U_1^j(\vartheta_1(t_1^j), \varphi_1 + \xi_1^j), \quad (41)$$

$$U_2(\tau_2) = \prod_{j=1}^N U_2^j(\vartheta_2 + \xi_2^j, \varphi_2(t_2^j)), \quad (42)$$

$$U_3(\tau_3) = \prod_{j=1}^N U_3^j(\vartheta_3(t_3^j), \varphi_3 + \xi_3^j), \quad (43)$$

where  $(j-1)\tau_i \leq t_i^j \leq j\tau_i$  and  $\xi_i^j \in [-\gamma, \gamma]$  are random variables uniformly distributed in the chosen interval. We stress again that each operator in the decomposition has a (large and not transparent) analytical expression. Using this model we have computed the average gate fidelity at the first optimal operational time  $\tau^*$  by means of Eq. (34) and averaging over 50 realizations of the random process. The result is shown in Fig. 4. In this plot we have rescaled the noise amplitude  $\gamma$  with the maximum value of the parameter for the loop in Fig. 1(b) (i.e.  $\pi/2$ ). Also for this model the fidelity exhibits a breakdown for small frequencies of the noise (which is in accordance with previous results). In particular, the value  $\tau^*/\tau_{\text{step}} \simeq 6.5$  exhibits the minimum value of  $F$  for any amplitude of the noise. Anyway, we notice that the deep of the fidelity is pronounced if the noise amplitude is one half the maximum value of the parameters; clearly, this situation corresponds to an unphysical scenario in which the control of the parameters is very poor. In all other situations the typical values of  $F$  is very high. In the range of intermediate and large frequencies  $F$  quickly recovers the ideal behavior.

It is interesting to compare the behavior of the gate at the first optimal operational time to the case of longer operational time in presence of noise, i.e., in the (approximated) adiabatic regime. It is possible to see [22, 23] that the fidelity oscillations shown in Fig. 2 in absence of noise are strongly suppressed if  $k \geq 3$  in Eq. (22) (we are near the adiabatic regime).

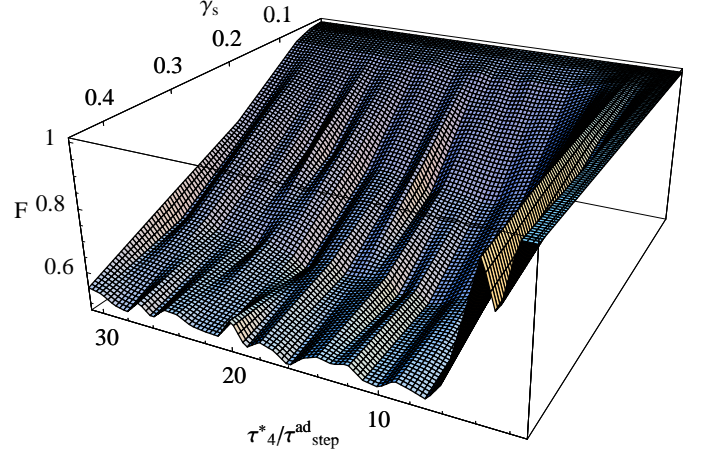


FIG. 5: (Color on line.) Average gate fidelity at the fourth optimal operational time as a function of the rescaled noise amplitude  $\gamma_s = \gamma/(\pi/2)$  and the ratio  $\tau_4^*/\tau_{\text{step}}^{\text{ad}}$  for the model in Sec. IV B.

Therefore, we have computed the average gate fidelity at the fourth optimal operational time, namely  $\Omega\tau_4^* \simeq 75.21$  (in this case  $\tau_{\text{step}}^{\text{ad}} = \tau_4^*/3N$ ). The result is shown in Fig. 5 and can be directly compared to the plot in Fig. 4. We notice that, in the same range of frequencies of the non adiabatic case,  $F$  reaches lower values. Moreover, the adiabatic gate needs higher values of the frequency of noise for recovering the ideal behavior. Therefore, the adiabatic (purely geometric) NOT transformation is more sensitive than to parametric noise than the non adiabatic one.

### C. Random noise

In this section we consider a model for a random perturbation of the loop which is not constrained to preserve the sphere in the parameter space. Taking in consideration the ideal loop (21) here we study the noisy paths of the following kind:

$$\begin{cases} x_n(s; \tau_{\text{step}}, \epsilon, \tau) = x(s) + \xi_1(s, \tau_{\text{step}}, \tau) \\ y_n(s; \tau_{\text{step}}, \epsilon, \tau) = y(s) + \xi_2(s, \tau_{\text{step}}, \tau) \\ z_n(s; \tau_{\text{step}}, \epsilon, \tau) = z(s) + \xi_3(s, \tau_{\text{step}}, \tau) \end{cases}, \quad (44)$$

where  $\xi_i(s, \tau_{\text{step}}, \tau) \in [-\epsilon, \epsilon]$  are three random variables, uniformly distributed in the chosen interval, which are piecewise constant for  $(j-1)\tau_{\text{step}} \leq s\tau \leq j\tau_{\text{step}}$ .

For the first optimal working time  $\tau = \tau^*$  we have numerically solved the noisy Schrödinger equation by means of the relation (35) for 50 realizations of the noise. The estimated average gate fidelity at the first optimal operational time is plotted in Fig. 6 as a function of the typical noise frequency for different values of the noise amplitude. This plot shows that even for this model of noise the same qualitative behavior of the average gate fidelity as a function of the noise typical frequency is found.

In order to compare the first optimal operational time to longer operational times in the noisy case, we have computed the average gate fidelity at the third optimal operational time,

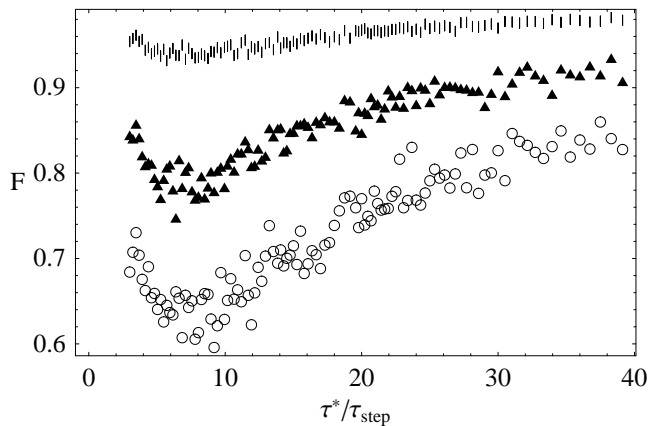


FIG. 6: Average gate fidelity at the first optimal operational time as a function of noise typical frequency for several value of the noise amplitude for the noise model in Sec. IV C. Dashes:  $\epsilon = 0.1\Omega$ ; triangles:  $\epsilon = 0.2\Omega$ ; circles:  $\epsilon = 0.3\Omega$ .

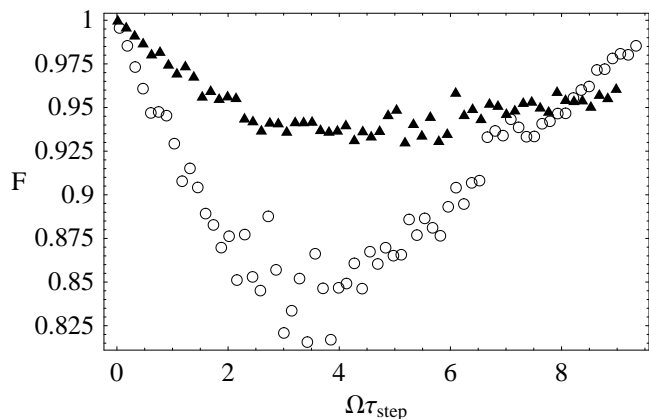


FIG. 7: Average gate fidelity as a function of noise typical time at the first (triangles) and the third (circles) optimal operational time for the noise model in Sec. IV C with amplitude  $\epsilon = 0.1\Omega$ .

namely  $\Omega\tau_3^* = 56.32$ . The results are showed in Fig. 7 where the average gate fidelity is plotted for both the first and the third optimal operational time as a function of the typical time of the noise  $\tau_{step}$ . The results are compatible with those for the model of noise in Sec. IV B in the sense that also in this case the first optimal operational time can be preferable to longer operational time.

## V. COMMENTS AND CONCLUSIONS

In this paper we have considered the influence of parametric noise on the efficiency of a non adiabatic holonomic gate

which is known to be robust in the ideal case. Three models of parametric noise have been discussed in the case of finite operational time.

The average gate fidelities for all the models of noise considered here present an analogous qualitative behavior. For each of the three models the non ideal gate presents a breakdown of the average gate fidelity for small frequencies of the noise, while a high value of the fidelity is reached for noise with higher frequencies.

This can lead to say that the presence of a “resonant frequency” for the breakdown of  $F$  is a general feature of any model of parametric noise. Despite these considerations, our calculations show that, at least in certain situations, the first optimal operational time can be preferable to longer operational times with regards to the robustness of the corresponding gate against parametric noise. Apparently the recover of the ideal fidelity is obtained for the non adiabatic gates for lower frequencies of the noise, showing that the optimal working point defined in [22] is robust also versus this kind of disturb.

We want to stress again that the usual argument in favor of the robustness of holonomic quantum computation is based on the purely geometric nature of the holonomy group that describes the adiabatic transformations. Since the geometric character is present only in the adiabatic limit, the robustness of adiabatic gates is, in this sense, just a consequence of the adiabatic theorem. Recently, a family of non adiabatic holonomic gates has been discussed that present an unit fidelity at finite time, far before the adiabatic limit is reached. Although the nature of these gates remains unclear at the moment, what we want to emphasize here is that the argument in favor of the robustness of holonomic gates cannot be simply extended to the case of non adiabatic gates since at finite operational time the adiabatic theorem cannot be applied.

In order to understand the relation between adiabatic and finite time holonomic gates in presence of parametric noise, a careful analysis of the adiabatic limit of noisy gates should be useful. Such an analysis could be compared to the results of [16] in which the noise is introduced *after* the adiabatic limit is reached.

There is also need to understand in what sense these non adiabatic gates can be consider holonomic, that is to say, what of the presented features of such gates can be extended to generic systems and what are strictly dependent on the considered case study.

[1] M. A. Nielsen, I. L. Chuang, *Quantum Computation and Quantum Information* (Cambridge University Press, Cambridge,

2000).

[2] G. Benenti, G. Casati and G. Strini, *Principles of Quantum*

- Computation and Information* (World Scientific, Singapore, 2004).
- [3] H. P. Breuer, F. Petruccione, *The Theory of Open quantum Systems* (Oxford University Press, Oxford, 2002).
- [4] D. J. Wineland, C. Monroe, W. M. Itano, D. Leibfried, B. E. King, D. M. Meekhof, J. Res. Natl. Inst. Stand. Technol. **103**, 259 (1998).
- [5] P. Zanardi, M. Rasetti, Phys. Lett. A **264**, 94 (1999).
- [6] J. Pachos, P. Zanardi and M. Rasetti, Phys. Rev. A **61**, 010305(R) (1999).
- [7] M. Nakahara, *Geometry, topology and physics*, 2nd Ed., (IoP publishing, Bristol, 2005).
- [8] K. B. Marathe, G. Martucci, *The Mathematical Foundations of Gauge Theories* (North-Holland, Amsterdam, 1992).
- [9] M. V. Berry, Proc. R. Soc. Lond. A **392**, 45 (1984); B. Simon, Phys. Rev. Lett. **51**, 2167 (1983).
- [10] F. Wilczek and A. Zee, Phys. Rev. Lett. **52**, 2111 (1984).
- [11] J. Pachos, P. Zanardi, Int. J. Mod. Phys. B **15**, 1257 (2001).
- [12] T. Kato, J. Phys. Soc. Jap. **5**, 435 (1951).
- [13] Y. Aharonov, J. Anandan, Phys. Rev. Lett. **58**, 1593 (1987).
- [14] J. Anandan, Phys. Lett. A **133**, 171 (1988).
- [15] G. De Chiara, G. M. Palma, Phys. Rev. Lett. **91**, 090404 (2003).
- [16] P. Solinas, P. Zanardi and N. Zanghì, Phys. Rev. A **70**, 042316 (2004).
- [17] A. Carollo, I. Fuentes-Guridi, M. França Santos and V. Vedral, Phys. Rev. Lett. **90**, 160402 (2003).
- [18] A. Carollo, I. Fuentes-Guridi, M. França Santos and V. Vedral, Phys. Rev. Lett. **92**, 020402 (2004).
- [19] I. Fuentes-Guridi, F. Girelli, E. Livine, Phys. Rev. Lett. **94**, 020503 (2005).
- [20] D. Parodi, M. Sassetti, P. Solinas, P. Zanardi, N. Zanghì, Phys. Rev. A **73**, 052304 (2006).
- [21] L.-A. Wu, P. Zanardi, D. A. Lidar, Phys. Rev. Lett. **95**, 130501 (2005).
- [22] G. Florio, P. Facchi, R. Fazio, V. Giovannetti and S. Pascazio, Phys. Rev. A **73**, 022327 (2006).
- [23] A. Trullo, P. Facchi, R. Fazio, G. Florio, V. Giovannetti, S. Pascazio, Las. Phys. **16**, 1478 (2006).
- [24] G. Florio, Open Sys. & Information Dyn. **13**, 263 (2006).
- [25] L.-M. Duan, J. I. Cirac, P. Zoller, Science **292**, 1695 (2001).
- [26] G. Falci, R. Fazio, G. M. Palma, J. Siewert and V. Vedral, Nature **407**, 355 (2000).
- [27] L. Faoro, J. Siewert and R. Fazio, Phys. Rev. Lett. **90**, 028301 (2003).
- [28] P. Solinas, P. Zanardi, N. Zanghì and F. Rossi, Phys. Rev. A **67**, 062315 (2003).
- [29] M. S. Sarandy, D. A. Lidar, Phys. Rev. Lett. **95**, 250503 (2005).
- [30] M. S. Sarandy, D. A. Lidar, Phys. Rev. A **71**, 012331 (2005); **73**, 062101 (2006).
- [31] M. Born and V. Fock, Z. Phys. **51**, 165 (1928).
- [32] M. A. Nielsen, Phys. Lett. A **303**, 249 (2002); M. D. Bowdrey, D. K. L. Oi, A. J. Short, K. Banaszek and J. A. Jones, *ibid.* **294**, 258 (2002); M. Horodecki, P. Horodecki and R. Horodecki, Phys. Rev. A **60**, 1888 (1999).
- [33] We recall that geometric phases arise also in the context of (non-adiabatic) cyclic evolutions [13, 14], but only *adiabatic* phases are relevant for our purposes.